

Generation of gravitational waves during early structure formation between cosmic inflation and reheating

Karsten Jedamzik*

*Laboratoire de Physique Théorique et Astroparticules, UMR 5207-CNRS,
Université de Montpellier II, F-34095 Montpellier, France*

Martin Lemoine[†] and Jérôme Martin[‡]

*Institut d'Astrophysique de Paris,
UMR 7095-CNRS, Université Pierre et Marie Curie,
98bis boulevard Arago, 75014 Paris, France*

(Dated: October 31, 2018)

In the pre-reheating era, following cosmic inflation and preceding radiation domination, the energy density may be dominated by an oscillating massive scalar condensate, such as is the case for $V = m^2\phi^2/2$ chaotic inflation. We have found in a previous paper that during this period, a wide range of sub-Hubble scale perturbations are subject to a preheating instability, leading to the growth of density perturbations ultimately collapsing to form non-linear structures. We compute here the gravitational wave signal due to these structures in the linear limit and present estimates for emission in the non-linear limit due to various effects: the collapse of halos, the tidal interactions, the evaporation during the conversion of the inflaton condensate into radiation and finally the ensuing turbulent cascades. The gravitational wave signal could be rather large and potentially testable by future detectors.

I. INTRODUCTION

One of the most salient features of inflationary cosmology is undoubtedly the generation of both scalar and tensor modes of metric perturbations on super-horizon scales through the amplification of vacuum fluctuations. Scalar modes correspond to genuine density fluctuations which are probed with ever increasing accuracy by the measurements of the temperature fluctuations of the cosmic microwave background and large scale surveys. Tensor modes, however remain to be detected. Current (e.g. Planck [1]) or next generation experiments (e.g. BBO [2], DECIGO [3]) should in principle detect the relic gravitational wave background if the energy scale of inflation is close to the GUT scale. As is well known, gravitational waves are much harder to detect because of the intrinsic weakness of gravity, but at the same time and for the same reason they offer an invaluable probe of early Universe physics.

In the past two decades, it has been realized that gravitational waves could also be produced in the primordial Universe and on sub-horizon scales due to a rapid disturbance of an otherwise equilibrium homogeneous state. This may occur for instance in first order primordial phase transitions [4–9], through bubble collisions and the dissipation of energy in turbulent cascades [10–12], or via the interactions of waves generated by parametric amplification in preheating scenarios involving multiple scalar fields or tachyonic couplings of the inflaton [13–18].

These various scenarios lead to different predictions at different frequencies depending on the detailed processes at work, with interesting prospects for detection [19].

In a previous paper (hereafter Paper I) [20], we have shown that *single field* inflation generically leads to the growth of density fluctuations in the pre-reheating era for a certain range of wave numbers on sub-Hubble scales, and we have argued that one of the possible signatures of this effect would be the generation of gravitational waves (GW). The objective of the present paper is to calculate explicitly the spectrum of gravitational waves emitted by the interactions of these density perturbations. In order to avoid unnecessary model dependencies, we focus on the simplest model of inflation, namely chaotic inflation with potential $V(\phi) = m^2\phi^2/2$. Then, the normalization of the density perturbation power spectrum to the value measured by cosmic microwave probes sets the scale for the mass m and the Hubble parameter at the end of inflation. The only parameter left in the model is the reheating temperature of the Universe, T_{rh} , which marks the beginning of the radiation dominated era and which is directly related to the decay constant Γ_ϕ of the inflaton, $T_{\text{rh}} \sim 0.2\sqrt{\Gamma_\phi M_{\text{Pl}}}$ (with M_{Pl} the reduced Planck mass). In the following, we calculate the present day gravitational wave spectrum in the linear regime and provide detailed estimates for gravitational wave emission due to non-linear effects, which are associated with the growth of the density contrast on different scales beyond unity. We find potentially observable signals, all the more so when the reheating temperature is lowered. A lower reheating temperature is associated with a longer epoch during which density fluctuations may grow as well as a frequency closer to the range of maximum sensitivity of next generation gravitational wave detectors.

Recently, the problem of gravitational wave emission

*Electronic address: jedamzik@lpta.univ-montp2.fr

[†]Electronic address: lemoine@iap.fr

[‡]Electronic address: jmartin@iap.fr

by the growth of density fluctuations in an early matter era has been discussed by Assadullahi and Wands [21]. The problem at hand is very similar but there are several differences between this study and the present one. Firstly, Assadullahi and Wands do not specify the mechanism through which fluctuations can grow but assume that all sub-horizon modes are unstable if the equation of state of the background field is on average pressure-less, as happens for $m^2\phi^2$ during the inflaton oscillatory phase. As demonstrated in Paper I however, growth of fluctuations is a preheating effect, which is limited to a band of wave numbers, whose range depends on the precise shape of the potential. Borrowing from this calculation, we are thus able in the present paper to relate the growth of fluctuations with the initial post-inflationary power spectrum of metric fluctuations. More importantly, we provide in the present paper detailed estimates for the non-linear regime of matter fluctuations, while the authors of Ref. [21] have focused their study only on the linear regime.

The outline of the paper is as follows: In Section II we recall the main findings of Paper I and set the stage for the calculation of the gravitational wave signal done in Section III in the linear limit. Section IV discusses in four subsections, gravitational wave emission in the non-linear regime, due to the first collapse phase of density fluctuations, due to the non-linear phases after first collapse, due to the evaporation of the collapsed halos at reheating and due to the dissipation of energy in turbulent cascades after reheating, respectively. Conclusions are drawn in Section V.

II. GRAVITATIONAL INSTABILITY IN THE PRE-REHEATING ERA

In this section, we briefly recall the main findings of Paper I. In that article, we have discussed the evolution of the Mukhanov variable $v_{\mathbf{k}}$ and of the curvature perturbation $\zeta_{\mathbf{k}}$ during the pre-heating epoch. These two variables control the dynamics of the scalar metric perturbations. During pre-heating, the inflaton field oscillates according to

$$\phi(t) \simeq \phi_{\text{end}} \left(\frac{a_{\text{end}}}{a} \right)^{3/2} \sin(mt), \quad (1)$$

where $\phi_{\text{end}} \simeq m_{\text{Pl}}/(2\sqrt{3})$ is the inflaton vacuum expectation value at the end of inflation, and where $m_{\text{Pl}} \equiv \sqrt{8\pi}M_{\text{Pl}}$. The mass m is fixed by the COBE/WMAP normalization, $m \simeq 1.7 \times 10^{13}$ GeV. The Mukhanov variable $v_{\mathbf{k}}$ is related to the curvature perturbation $\zeta_{\mathbf{k}}$ by

$$\zeta_{\mathbf{k}} = \sqrt{\frac{\kappa}{2}} \frac{v_{\mathbf{k}}}{a\sqrt{\epsilon_1}}, \quad (2)$$

where $\epsilon_1 \equiv -\dot{H}/H^2$ is the first slow-roll parameter expressed in terms of the Hubble parameter $H = \dot{a}/a$. The

quantity a denotes the Friedman-Lemaître-Robertson-Walker scale factor, $\kappa \equiv M_{\text{Pl}}^{-2}$ and a dot means a derivative with respect to cosmic time.

In Paper I, we have shown that there exists an instability regime of narrow resonance provided the wave number of the Fourier mode is such that

$$0 < \frac{k}{a} < \sqrt{3Hm}. \quad (3)$$

Once a mode has entered this resonance band, it remains inside it during the whole oscillatory phase. Moreover, we have also demonstrated that, in the resonance band, $v_{\mathbf{k}} \propto a$ and, therefore, given the definition of this quantity given above, that $\zeta_{\mathbf{k}}$ remains constant. Note that usually the curvature perturbation remains constant only on super Hubble scales while decaying on sub Hubble scales, unless there is gravitational instability. By using the perturbed Einstein equation

$$\delta_{\mathbf{k}} = -\frac{2}{5} \left(\frac{k^2}{a^2 H^2} + 3 \right) \zeta_{\mathbf{k}}, \quad (4)$$

with the shorthand notation $\delta_{\mathbf{k}}(\eta) \equiv \delta\rho_{\mathbf{k}}/\rho$ introducing the fractional mass-energy density perturbation, and given that $\rho \propto 1/a^3$, we may see that $\delta_{\mathbf{k}}$ grows as $a(t)$ on sub-Hubble scales and remains constant on super-Hubble scales. The preheating instability for all sub-Hubble modes with $k/a < \sqrt{3Hm}$ may be understood as the gravitational instability of the oscillating scalar condensate.

As already stated, the amplification described above occurs only for a limited range of scales, $k \in [k_{\text{min}}, k_{\text{max}}]$ in terms of comoving wave number. We now discuss this point in more detail and specify k_{min} and k_{max} . A priori, the smallest unstable scale (in wavelength) is that which enters the resonance band at the end of reheating. However, it has never been outside the Hubble scale during inflation and, therefore, the power stored on that scale at the end of inflation is suppressed. As a consequence, for practical purposes, one can consider that the smallest scale for which the amplification occurs is such that $k \simeq a_{\text{end}}H_{\text{end}}$, i.e. $\hat{k} \equiv k/(a_{\text{end}}H_{\text{end}}) \simeq 1$, describing modes that leave and re-enter immediately the Hubble radius at the end of inflation, hence $k_{\text{max}} = a_{\text{end}}H_{\text{end}}$ ($\hat{k}_{\text{max}} = 1$). More detail on this issue can also be found in paper I.

On the other hand, the largest scale is the one for which modes re-enter the Hubble radius at the end of the matter dominated pre-reheating epoch, i.e. $k_{\text{min}} \simeq a_{\text{rh}}H_{\text{rh}}$, where H_{rh} is the Hubble parameter at the end of the reheating epoch or at the beginning of the radiation dominated phase. One can show that the number of e-folds between the Hubble radius exit of k_{min} during inflation and the end of inflation is formally given by:

$$\ln \left(\frac{a_{\text{end}}}{a_{k_{\text{min}}}} \right) = -\frac{1}{2} - \frac{1}{2} W_{-1} \left(-e^{-1} \hat{k}_{\text{min}}^2 \right), \quad (5)$$

where W_{-1} denotes the Lambert function. If one neglects the evolution of the Hubble scale over the interval between Hubble radius exit of k_{min} and the end of inflation,

the above can be approximated with $a_{k_{\min}}/a_{\text{end}} \simeq \hat{k}_{\min}$. In terms of the reheating temperature and inflationary scale given by

$$\begin{aligned} \hat{k}_{\min} &= \frac{a_{\text{rh}} H_{\text{rh}}}{a_{\text{end}} H_{\text{end}}} \\ &\simeq 5.9 \times 10^{-5} \left(\frac{T_{\text{rh}}}{10^9 \text{ GeV}} \right)^{2/3}. \end{aligned} \quad (6)$$

The last equation assumes $g_* = 230$ degrees of freedom at reheating. For a reheating temperature of $T_{\text{rh}} \simeq 10^9$ GeV, one finds $\ln(a_{\text{end}}/a_{k_{\min}}) \simeq 11$. Therefore, for $T_{\text{rh}} \simeq 10^9$ GeV, the scales we would be interested in in this article are those which left the Hubble radius during inflation between eleven and zero e-folds before the end of inflation.

Finally, we also need the initial power stored on each scale $k \in [k_{\min}, k_{\max}]$ at the end of inflation. This is described by the power spectrum of the curvature fluctuation defined by

$$\mathcal{P}_\zeta(k) \equiv \frac{k^3}{2\pi^2} |\zeta_{\mathbf{k}}|^2 = \frac{2k^3}{\pi m_{\text{pl}}^2} \left| \frac{v_{\mathbf{k}}}{a\sqrt{\epsilon_1}} \right|^2. \quad (7)$$

The corresponding primordial power spectrum for $m^2\phi^2/2$ inflation correctly normalized to COBE/WMAP observations is shown in Fig. 1. This figure has been obtained through a numerical integration of the evolution of $\zeta_{\mathbf{k}}$ (through $v_{\mathbf{k}}$): as discussed in Paper I, the slow-roll approximation at first or even second order cannot reliably predict the shape of the power spectrum in the range of comoving wave numbers of interest to us, $k \lesssim a_{\text{end}} H_{\text{end}}$, which exit and re-enter the Hubble radius not too long afterward (in particular, before reheating is completed). In the notation of Fig. 1, $N_{\text{exit}} - N_{\text{end}} \sim -10 \rightarrow 0$, the lower bound depending on the exact value of the reheating temperature.

III. GENERATION OF GRAVITATIONAL WAVES AFTER INFLATION: THE LINEAR REGIME

Let us now consider the production of GWs induced by the phenomenon described in the previous section. Our analysis follows the main thread of the analysis presented in Refs. [10, 18]. We work with the metric

$$ds^2 = a^2 \{ (1 + 2\Phi) d\eta^2 - [(1 + 2\Phi)\delta_{ij} + h_{ij}] dx_i dx_j \}, \quad (8)$$

where Φ is the gauge-invariant potential (*i.e.* the potential in longitudinal gauge) which describes the presence of inhomogeneities in the inflaton field and h_{ij} is the transverse traceless spatial tensor accounting for the generation of GWs. We are interested in the amplitude h_{ij} of the transverse and traceless which obey the following equation (in Fourier space)

$$\bar{h}_{ij}'' + \left(k^2 - \frac{a''}{a} \right) \bar{h}_{ij} = 2\kappa a T_{ij}^{\text{TT}}(\eta, \mathbf{k}), \quad (9)$$

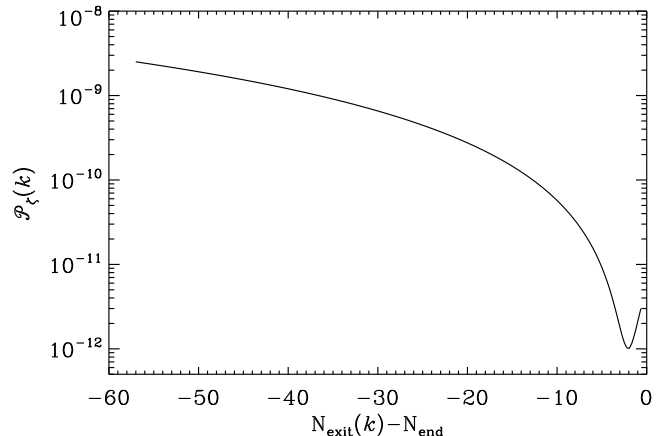


FIG. 1: Primordial power spectrum of curvature perturbations for the large field inflation model with $V(\phi) = m^2\phi^2/2$. Here $N_{\text{exit}}(k) - N_{\text{end}}$ is $\ln[a_{\text{cross}}(k)/a_{\text{end}}]$, with $a_{\text{cross}}(k)$ the scale factor at Hubble radius crossing of mode k during inflation and a_{end} the scale factor at the end of inflation.

where we used the rescaled amplitude $\bar{h}_{ij} = ah_{ij}$ and with $T_{ij}(\eta, \mathbf{k}) = \int d\mathbf{x} e^{i\mathbf{k}\cdot\mathbf{x}} T_{ij}(\eta, \mathbf{x}) / (2\pi)^{3/2}$. The transverse traceless part of the spatial energy-momentum tensor T_{ij}^{TT} is obtained by

$$T_{ij}^{\text{TT}} \equiv \perp_{ij\ell m} T_{\ell m}, \quad (10)$$

with

$$\perp_{ij\ell m} \equiv P_{i\ell}(\mathbf{e}_{\mathbf{k}}) P_{jm}(\mathbf{e}_{\mathbf{k}}) - \frac{1}{2} P_{ij}(\mathbf{e}_{\mathbf{k}}) P_{\ell m}(\mathbf{e}_{\mathbf{k}}), \quad (11)$$

and

$$P_{ij}(\mathbf{e}_{\mathbf{k}}) \equiv \delta_{ij} - e_{\mathbf{k},i} e_{\mathbf{k},j}. \quad (12)$$

Here the quantity $\mathbf{e}_{\mathbf{k}} \equiv \mathbf{k}/k$ is the unit vector in the \mathbf{k} direction. We are interested in the generation of GWs by the parametrically growing inflaton density perturbations between the end of inflation and the epoch of reheating, *i.e.* the epoch of inflaton decay. We will see below that the lowest non-vanishing contribution of these perturbations to T_{ij}^{TT} appears only at second order in the perturbative quantity $\delta_{\mathbf{k}}$. We will thus work to this order in T_{ij}^{TT} but only to first order in all other quantities. If we neglect the term a''/a , as appropriate for sub Hubble scales, then the solution of the above equation can be written as

$$\bar{h}_{ij}(\eta, \mathbf{k}) = A_{ij}(\mathbf{k}) \sin[k(\eta - \eta_{\text{f}})] + B_{ij}(\mathbf{k}) \cos[k(\eta - \eta_{\text{f}})], \quad (13)$$

where

$$A_{ij} = \frac{2\kappa}{k} \int_{\eta_{\text{ini}}}^{\eta_{\text{f}}} d\tau \cos[k(\eta_{\text{f}} - \tau)] a(\tau) T_{ij}^{\text{TT}}(\tau, \mathbf{k}), \quad (14)$$

$$B_{ij} = \frac{2\kappa}{k} \int_{\eta_{\text{ini}}}^{\eta_{\text{f}}} d\tau \sin[k(\eta_{\text{f}} - \tau)] a(\tau) T_{ij}^{\text{TT}}(\tau, \mathbf{k}). \quad (15)$$

In these expression, we have assumed that the source is non negligible in the time interval $\eta_{\text{ini}} < \eta < \eta_{\text{f}}$. In our calculation, the initial time is set by the time at which a given mode enters the Hubble radius, while η_{f} is given

by the time at which a mode reaches non-linearity. A discussion of generation of GWs in the non-linear regime is deferred to the next section. The energy density of GWs is given by

$$\rho_{\text{gw}}(\eta) = \frac{1}{4\kappa a^4(\eta)} \sum_{ij} \langle \bar{h}'_{ij}(\eta, \mathbf{x}) \bar{h}'_{ij}(\eta, \mathbf{x}) \rangle . \quad (16)$$

where terms proportional to the Hubble constant have been neglected, appropriate for $k/a \gg H$. Using the Fourier expansion, one obtains

$$\begin{aligned} \rho_{\text{gw}}(\eta) = & \frac{1}{4\kappa a^4(\eta)} \sum_{ij} \int \frac{d\mathbf{k}}{(2\pi)^{3/2}} \int \frac{d\mathbf{k}'}{(2\pi)^{3/2}} e^{-i(\mathbf{k}-\mathbf{k}')\cdot\mathbf{x}} k k' \left\{ \langle A_{ij}(\mathbf{k}) A_{ij}^*(\mathbf{k}') \rangle \cos[k(\eta - \eta_{\text{f}})] \cos[k'(\eta - \eta_{\text{f}})] \right. \\ & - \langle A_{ij}(\mathbf{k}) B_{ij}^*(\mathbf{k}') \rangle \cos[k(\eta - \eta_{\text{f}})] \sin[k'(\eta - \eta_{\text{f}})] - \langle B_{ij}(\mathbf{k}) A_{ij}^*(\mathbf{k}') \rangle \sin[k(\eta - \eta_{\text{f}})] \cos[k'(\eta - \eta_{\text{f}})] \\ & \left. + \langle B_{ij}(\mathbf{k}) B_{ij}^*(\mathbf{k}') \rangle \sin[k(\eta - \eta_{\text{f}})] \sin[k'(\eta - \eta_{\text{f}})] \right\} . \end{aligned} \quad (17)$$

where we have also used $A_{ij}(\mathbf{k}) = A_{ij}^*(-\mathbf{k})$ and $B_{ij}(\mathbf{k}) = B_{ij}^*(-\mathbf{k})$ imposed by $h_{ij}(\eta, \mathbf{x})$ being real. Expression Eq. (17) contains four terms. Let us first discuss the first one. One needs to express the correlator of two coefficients A_{ij} . Using the expressions established before, see Eq. (14), one is led to

$$\langle A_{ij}(\mathbf{k}) A_{ij}^*(\mathbf{k}') \rangle = \frac{4\kappa^2}{kk'} \int_{\eta_{\text{ini}}}^{\eta_{\text{f}}} d\tau \int_{\eta_{\text{ini}}}^{\eta_{\text{f}}} d\tau' \cos[k(\eta_{\text{f}} - \tau)] \cos[k'(\eta_{\text{f}} - \tau')] a(\tau) a(\tau') \langle T_{ij}^{\text{TT}}(\tau, \mathbf{k}) T_{ij}^{\text{TT}*}(\tau', \mathbf{k}') \rangle , \quad (18)$$

where one has

$$\langle T_{ij}^{\text{TT}}(\tau, \mathbf{k}) T_{ij}^{\text{TT}*}(\tau', \mathbf{k}') \rangle = \perp_{ij\ell m} \perp_{ijrs} \langle T_{\ell m}(\tau, \mathbf{k}) T_{rs}^*(\tau', \mathbf{k}') \rangle , \quad (19)$$

with the projectors defined in Eqs. (11) and (12).

To go further, one needs to specify what the stress-energy tensor is. We take the stress-energy tensor of a pressure-less fluid since, when the field rapidly oscillates at the bottom of its potential, the pressure vanishes on average. Therefore, we have

$$T_{ij} = \rho a^2 v_i v_j , \quad (20)$$

where \mathbf{v} represents the velocity of the particles in the pressure-less fluid. Note that Eq. (20) is already second order in the perturbation since v_i is first order. The velocity can be calculated from the continuity equation which reads

$$\frac{\partial}{\partial t} \left(\frac{\delta\rho}{\rho} \right) + \frac{1}{a} \nabla \cdot \mathbf{v} = 0 . \quad (21)$$

Fourier transforming Eq. (21), and noting that $\delta\rho_{\mathbf{k}}/\rho \propto a(t)$ for growing density fluctuations in which we are interested (as was discussed in the previous section), we may relate the Fourier amplitudes of density perturbation and velocity via

$$\mathbf{v}(\eta, \mathbf{k}) = -\frac{iHa}{k} \delta_{\mathbf{k}}(\eta) \mathbf{e}_{\mathbf{k}} . \quad (22)$$

Then, inserting the above expression for the velocity into the definition of the stress-energy tensor Fourier component, one obtains that

$$\begin{aligned} \langle T_{\ell m}(\tau, \mathbf{k}) T_{rs}^*(\tau', \mathbf{k}') \rangle = & \frac{1}{(2\pi)^3} \rho(\tau) a^4(\tau) H^2(\tau) \rho(\tau') a^4(\tau') H^2(\tau') \int d\mathbf{q} \int d\mathbf{p} \frac{q\ell(k_m - q_m)}{q^2(k - q)^2} \frac{p_r(k'_s - p_s)}{p^2(k' - p)^2} \\ & \times \langle \delta_{\mathbf{q}}(\tau) \delta_{\mathbf{k}-\mathbf{q}}(\tau) \delta_{\mathbf{p}}^*(\tau') \delta_{\mathbf{k}'-\mathbf{p}}^*(\tau') \rangle . \end{aligned} \quad (23)$$

Then we use the fact that the density contrast grows proportional to a when the mode is inside the Hubble radius, while it remains constant from the end of inflation until Hubble radius crossing. Therefore, in the sub-horizon regime, one can write $\delta_{\mathbf{q}}(\tau) = \delta_{\mathbf{q}}(\tau_{\text{end}})a(\tau)/a_{\text{hc}}$, with a_{hc} the scale factor at horizon crossing and $\delta_{\mathbf{q}}(\tau_{\text{end}})$ the value of $\delta_{\mathbf{q}}$ at the end of inflation. In order to match both asymptotic behaviors in the super-horizon, namely $\delta_{\mathbf{q}}(\tau) \rightarrow \delta_{\mathbf{q}}(\tau_{\text{end}}) = (6/5)\zeta_{\mathbf{q}}$ and in the sub-horizon regimes, $\delta_{\mathbf{q}}(\tau) \rightarrow (2/5)[q/(aH)]^2 \zeta_{\mathbf{q}}$, see Eq. (4), one defines a_{hc} as that at which $q = \sqrt{3}a_{\text{hc}}H_{\text{hc}}$. Given that $aH \propto a^{-1/2}$ in this preheating stage, this indeed implies that $[q/(aH)]^2 = 3(a/a_{\text{hc}})$, hence the two asymptotes are matched at $a = a_{\text{hc}}$. Hence, one can write

$$\langle T_{\ell m}(\tau, \mathbf{k}) T_{rs}(\tau', \mathbf{k}') \rangle = \frac{1}{(2\pi)^3} \frac{1}{(3\kappa)^2} \int d\mathbf{q} \int d\mathbf{p} q_{\ell}(k_m - q_m) p_r(k'_s - p_s) \langle \delta_{\mathbf{q}}(\tau_{\text{end}}) \delta_{\mathbf{k}-\mathbf{q}}(\tau_{\text{end}}) \delta_{\mathbf{p}}^*(\tau_{\text{end}}) \delta_{\mathbf{k}'-\mathbf{p}}^*(\tau_{\text{end}}) \rangle, \quad (24)$$

The next step consists in evaluating the correlator. Using the Wick theorem in order to express the four-point correlation function in terms of three two-point correlations functions and discarding a homogeneous piece we are not interested in, one arrives at

$$\langle T_{\ell m}(\tau, \mathbf{k}) T_{rs}(\tau', \mathbf{k}') \rangle = \frac{2}{(2\pi)^3} \frac{1}{(3\kappa)^2} \int d\mathbf{q} q_{\ell}(k_m - q_m) q_r(k'_s - q_s) \sigma_q^2 \sigma_{|\mathbf{k}-\mathbf{q}|}^2 \delta(\mathbf{k} - \mathbf{k}'), \quad (25)$$

where we have defined $\langle \delta_{\mathbf{k}}(\tau_{\text{end}}) \delta_{\mathbf{k}'}^*(\tau_{\text{end}}) \rangle \equiv \sigma_{\mathbf{k}}^2 \delta(\mathbf{k} - \mathbf{k}')$. Finally, we act with the projectors on the last expression and one obtains

$$\sum_{ij} \langle T_{ij}^{\text{TT}}(\tau, \mathbf{k}) T_{ij}^{\text{TT}*}(\tau', \mathbf{k}') \rangle = \frac{1}{(2\pi)^3} \frac{1}{(3\kappa)^2} \int d\mathbf{q} q^4 \sin^4 \alpha \sigma_q^2 \sigma_{|\mathbf{k}-\mathbf{q}|}^2 \delta(\mathbf{k} - \mathbf{k}'), \quad (26)$$

where α is the angle between the vectors \mathbf{k} and \mathbf{q} . Putting everything together, one can therefore evaluate the correlator between the coefficients A_{ij} . We find

$$\begin{aligned} \sum_{ij} \langle A_{ij}(\mathbf{k}) A_{ij}^*(\mathbf{k}') \rangle &= \frac{4\kappa^2}{kk'} \int_{\eta_{\text{ini}}}^{\eta_{\text{f}}} d\tau \int_{\eta_{\text{ini}}}^{\eta_{\text{f}}} d\tau' a(\tau) \cos[k(\eta_{\text{f}} - \tau)] a(\tau') \cos[k'(\eta_{\text{f}} - \tau')] \frac{1}{(2\pi)^3} \frac{1}{(3\kappa)^2} \\ &\times \int d\mathbf{q} q^4 \sin^4 \alpha \sigma_q^2 \sigma_{|\mathbf{k}-\mathbf{q}|}^2 \delta(\mathbf{k} - \mathbf{k}'). \end{aligned} \quad (27)$$

Therefore, the first term in Eq. (17) is given by

$$\begin{aligned} \rho_{\text{gw}}^{\langle AA \rangle}(\eta) &= \frac{\kappa}{a^4(\eta)} \int \frac{d\mathbf{k}}{(2\pi)^3} \cos^2[k(\eta - \eta_{\text{f}})] \int_{\eta_{\text{ini}}}^{\eta_{\text{f}}} d\tau \int_{\eta_{\text{ini}}}^{\eta_{\text{f}}} d\tau' a(\tau) \cos[k(\eta_{\text{f}} - \tau)] a(\tau') \cos[k(\eta_{\text{f}} - \tau')] \\ &\times \frac{1}{(2\pi)^3} \frac{1}{(3\kappa)^2} \int d\mathbf{q} q^4 \sin^4 \alpha \sigma_q^2 \sigma_{|\mathbf{k}-\mathbf{q}|}^2. \end{aligned} \quad (28)$$

Taking the time average of the previous expression over a period replaces $\cos^2[k(\eta - \eta_{\text{f}})]$ with $1/2$, and cancels the cross-terms $\langle AB^* \rangle$, $\langle BA^* \rangle$. The term $\rho_{\text{gw}}^{\langle BB \rangle}$ is similar to $\rho_{\text{gw}}^{\langle AA \rangle}$ except that the term $\cos[k(\eta_{\text{f}} - \tau)] \cos[k'(\eta_{\text{f}} - \tau')]$ is replaced by $\sin[k(\eta_{\text{f}} - \tau)] \sin[k'(\eta_{\text{f}} - \tau')]$. When combined, these two terms lead to a present day energy density

$$\begin{aligned} \rho_{\text{gw}}(\tau_0) &= \frac{\kappa}{2(2\pi)^6 a_0^4} \int d\mathbf{k} \int_{\eta_{\text{ini}}}^{\eta_{\text{f}}} d\tau \int_{\eta_{\text{ini}}}^{\eta_{\text{f}}} d\tau' \cos[k(\tau - \tau')] a(\tau) a(\tau') \frac{1}{(3\kappa)^2} \\ &\times \int d\mathbf{q} q^4 \sin^4 \alpha \sigma_q^2 \sigma_{|\mathbf{k}-\mathbf{q}|}^2 = \frac{1}{(2\pi)^5 9\kappa a_0^4} \int dk k^2 \mathcal{J}(k) \mathcal{I}(k), \end{aligned} \quad (29)$$

where the functions \mathcal{J} and \mathcal{I} are defined as follows

$$\mathcal{J}(k) \equiv \int_{\eta_{\text{ini}}}^{\eta_{\text{f}}} d\tau \int_{\eta_{\text{ini}}}^{\eta_{\text{f}}} d\tau' \cos[k(\tau - \tau')] a(\tau) a(\tau'), \quad \mathcal{I}(k) \equiv \int d\mathbf{q} q^4 \sin^4 \alpha \sigma_q^2 \sigma_{|\mathbf{k}-\mathbf{q}|}^2. \quad (30)$$

The first integral can be done exactly. The result reads

$$\begin{aligned} \mathcal{J}(k) &= \frac{1}{16H_{\text{end}}^2} \left(\frac{k}{a_{\text{end}} H_{\text{end}}} \right)^{-6} \left\{ 8 + x_{\text{f}}^4 + x_{\text{ini}}^4 - \right. \\ &\quad \left. 2[4 + 4x_{\text{f}} x_{\text{ini}} - 2x_{\text{ini}}^2 + x_{\text{f}}^2 (x_{\text{ini}}^2 - 2)] \cos(x_{\text{f}} - x_{\text{ini}}) + 4(x_{\text{ini}} - x_{\text{f}}) (2 + x_{\text{f}} x_{\text{ini}}) \sin(x_{\text{f}} - x_{\text{ini}}) \right\}, \end{aligned} \quad (31)$$

with $x \equiv 3t_{\text{end}}^{2/3}t^{1/3}k/a_{\text{end}} = 2(a/a_{\text{end}})^{1/2}k/(a_{\text{end}}H_{\text{end}})$. Note that $x > 1$ for sub-Hubble modes. The second integral reads

$$\mathcal{I}(k) = 2\pi \int_{q_{\text{min}}}^{q_{\text{max}}} dq \int_{-1}^{+1} d\mu \sigma_q^2 \sigma_{|k-q|}^2 (1-\mu^2)^2 q^6. \quad (32)$$

Using $\delta_{\mathbf{q}}(\tau_{\text{end}}) = (6/5)\zeta_{\mathbf{q}}$ and Eq. (7), we have

$$\sigma_q^2 = \frac{36}{25} \frac{2\pi^2}{q^3} \mathcal{P}_\zeta(q), \quad (33)$$

where the power spectrum of the curvature perturbation is calculated at the end of inflation, see Fig. 1. As a consequence, one obtains

$$\mathcal{I}(k) = 8\pi^5 \left(\frac{36}{25}\right)^2 \int_{q_{\text{min}}}^{q_{\text{max}}} dq \int_{-1}^{+1} d\mu \mathcal{P}_\zeta(q) \mathcal{P}_\zeta\left(\sqrt{q^2 + k^2 - 2kq\mu}\right) \frac{(1-\mu^2)^2 q^3}{(q^2 + k^2 - 2kq\mu)^{3/2}}. \quad (34)$$

Using the above expressions, one finally obtains the present day contribution of these GWs to the critical density, *i.e.* $d\Omega_{\text{gw}}/d \ln k = \kappa/(3H_0^2) d\rho_{\text{gw},0}/d \ln k$

$$\frac{d\Omega_{\text{gw}}}{d \ln k} = \frac{12}{625} \left(\frac{a_{\text{end}}}{a_0}\right)^4 \left(\frac{H_{\text{end}}}{H_0}\right)^2 \left(\frac{a_{\text{rh}}}{a_{\text{end}}}\right)^2 \hat{k} \hat{\mathcal{J}}(\hat{k}) \hat{\mathcal{I}}(\hat{k}), \quad (35)$$

recalling the definitions introduced before: $\hat{k} \equiv k/(a_{\text{end}}H_{\text{end}})$, $\hat{q} \equiv q/(a_{\text{end}}H_{\text{end}})$ and introducing the dimensionless quantities

$$\hat{\mathcal{J}}(\hat{k}) \equiv 16H_{\text{end}}^2 x_{\text{f}}^{-4} \hat{k}^6 \mathcal{J}(k) = H_{\text{end}}^2 \hat{k}^2 \left(\frac{a_{\text{rh}}}{a_{\text{end}}}\right)^{-2} \mathcal{J}(k), \quad (36)$$

$$\hat{\mathcal{I}}(\hat{k}) \equiv \int_{\hat{q}_{\text{min}}}^{\hat{q}_{\text{max}}} d\hat{q} \int_{-1}^{+1} d\mu \mathcal{P}_\zeta(q) \mathcal{P}_\zeta\left(\sqrt{q^2 + k^2 - 2kq\mu}\right) \frac{(1-\mu^2)^2 \hat{q}^3}{(\hat{q}^2 + \hat{k}^2 - 2\hat{k}\hat{q}\mu)^{3/2}}, \quad (37)$$

where, in the argument of the power spectrum, q and k must be considered as function of \hat{q} and \hat{k} according to the simple relations introduced above.

Expression Eq. (35) may be further simplified when assuming a standard thermal history, *i.e.* radiation domination between the reheating epoch and the epoch of matter radiation-equality shortly before recombination. In this case

$$\frac{d\Omega_{\text{gw}}}{d \ln k} \simeq 2.8 \times 10^{-16} \Omega_{\gamma,0} \left(\frac{T_{\text{rh}}}{10^9 \text{GeV}}\right)^{-4/3} \times \hat{k} \hat{\mathcal{J}}(\hat{k}) \hat{\mathcal{I}}_{11}(\hat{k}), \quad (38)$$

where $\Omega_{\gamma,0} \simeq 5 \times 10^{-5}$ is the present density parameter in radiation and where we have defined $\mathcal{I}_{11}(\hat{k})$ by $\mathcal{I}_{11}(\hat{k}) \equiv 10^{22} \mathcal{I}(\hat{k})$ since $\mathcal{I}(\hat{k})$ is quadratic in \mathcal{P}_ζ . When reheating occurs long after the end of inflation, *i.e.* for $x_{\text{f}} \approx x_{\text{rh}} \gg x_{\text{ini}} \approx x_{\text{end}}$ which implies $a_{\text{rh}} \gg a_{\text{end}}$, the expression in the curly brackets of Eq. (31) approaches asymptotically x_{rh}^4 . In this case $\hat{\mathcal{J}}$ approaches unity.

Finally, it may also be interesting to have an expression giving the associated present day GW frequency. One

finds

$$f_0 \simeq 5 \times 10^5 \text{Hz} \hat{k} \left(\frac{T_{\text{rh}}}{10^9 \text{GeV}}\right)^{1/3}. \quad (39)$$

In Fig. 2, we show the result of a numerical integration of the above formula for two different reheating temperatures $T_{\text{rh}} = 10^9 \text{GeV}$ and $T_{\text{rh}} = 10^7 \text{GeV}$, respectively, along with projected sensitivities of next generation gravitational wave experiments, namely advanced LIGO [22, 23], BBO [2] and DECIGO [3]. The prediction for the above gravitational wave signal is shown by the thick solid line. At this stage, it is important to stress that the above calculation is carried out in the linear approximation and cannot describe the non-linear aspects. In particular, there exists a range of modes $[k_{\text{nl}}, k_{\text{max}}]$ for which growth is sufficiently effective that these modes become non-linear by the time reheating starts. This range of wave numbers is discussed in the next Section. Here, we wish to stress that the linear growth $\delta_{\mathbf{k}} \propto a$, as used in the above calculation, is not adequate anymore in the non-linear regime. This has impact on the above calculation in the range $[k_{\text{nl}}, k_{\text{max}}]$. In order to show how the calculation could be affected, we have plotted in thick

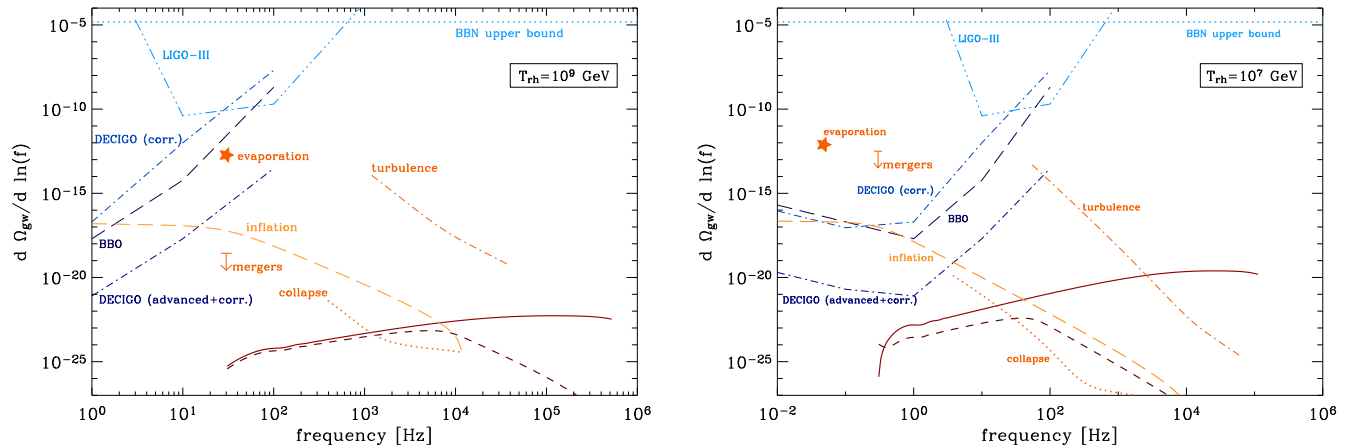


FIG. 2: Energy density in gravitational waves (in unit of the present day critical density) as a function of frequency. Left panel: $T_{\text{rh}} = 10^9$ GeV; right panel: $T_{\text{rh}} = 10^7$ GeV. The thick solid line shows the result of the linear calculation of the GW signal. The thick short dashed line shows the same calculation, but when stopped at the onset of the non-linear stage (see text). Various non-linear signal (discussed in Section IV) are shown: the dotted line (“collapse”) shows the signal associated with the collapse of halos that have gone non-linear by reheating; the upper limit “merger” presents an estimate of the possible amplification of the collapse signal due to tidal interactions; the dashed-dotted line (“turbulence”) shows the signal expected from the turbulence produced by the evaporation of non-linear structures at reheating; and the star symbol (“evaporation”) shows the signal produced by the evaporation of the collapsed halos at reheating. The long dashed line annotated “inflation” shows the signal expected from the direct generation of GWs in $m^2\phi^2$ inflation. On the left hand side, the various lines indicate the projected sensitivities of next generation gravitational wave detectors. The horizontal dotted line gives the limit imposed by big-bang nucleosynthesis.

dashed line in Fig. 2 the result obtained when one shuts off the emission of gravitational waves when mode k or $|\mathbf{k} - \mathbf{q}|$ become non-linear. This curve, which sets a strict lower limit to the gravitational wave signal departs from the above linear calculation in the range $[k_{\text{nl}}, k_{\text{max}}]$.

In Fig. 2, we also plot several estimates of gravitational wave production in the non-linear regime, to be discussed in Section IV. We also plot the signal expected from the direct production of gravitational waves in $m^2\phi^2$ inflation (represented as the long dashed line annotated “inflation”). We have calculated this signal following the study of [24]. The change of spectral evolution (from nearly scale invariant at small frequencies to $\propto k^{-2}$) occurs at a frequency $k_{\text{min}}/(2\pi)$, with $k_{\text{min}} = a_{\text{rh}}H_{\text{rh}}$. Indeed, modes with $k > k_{\text{min}}$ have re-entered the Hubble radius during inflaton domination in the pre-reheating epoch and suffered redshifting while those modes with $k < k_{\text{min}}$ have re-entered the horizon in the radiation dominated era (up to the modes with very small k that re-enter in the matter dominated era after matter-radiation equality, of course).

It is clear that the magnitude of the linear signal is weak for the reheating temperatures considered here. It is important to recall, however, that such reheating temperatures lie in the upper range of constraints set by the impact of gravitinos on big-bang nucleosynthesis and that in the absence of a definite underlying particle physics model in the inflaton sector, there is no particular scale for T_{rh} . The reheating temperature could be much lower, in which case the strength of the signal would increase

(roughly as $T_{\text{rh}}^{-4/3}$, see above) and the frequency would decrease (as $T_{\text{rh}}^{1/3}$), coming closer to the range of maximum sensitivity of future instruments.

IV. GENERATION OF GRAVITATIONAL WAVES IN THE NON-LINEAR REGIME

A. Collapse of halos

After perturbations have grown in the linear regime to $\delta\rho_k/\rho \sim 1$ they separate from the Hubble flow and collapse to form halos. In order to calculate the gravitational wave signal coming from this phase, we assume that the halos collapse and virialize instantaneously when the fluctuation on the scale considered exceeds the threshold $\delta_c \simeq 1.7$. With this approximation, a halo of mass M emits gravitational waves at a well-defined time and at a single pulsation $2\pi f$, which is estimated as the reciprocal of the dynamical timescale of collapse t_{coll} .

The energy density emitted during the collapse of perturbations corresponding to mass between M and $M + dM$ is

$$d\rho_{\text{gw}}^{\text{coll}} \simeq dn_{\text{h}}^{\text{coll}} \mathcal{L}_{\text{gw}}^{\text{coll}} t_{\text{coll}} \left(\frac{a_{\text{coll}}}{a_0} \right)^4. \quad (40)$$

In this expression, $\mathcal{L}_{\text{gw}}^{\text{coll}}$ is the luminosity emitted by one halo of mass M at collapse, $dn_{\text{h}}^{\text{coll}}$ represents the number

density of halos of mass between M and $M + dM$ at the time of collapse, and $t_{\text{coll}} \simeq (\kappa \rho_{\text{h}}/3)^{-1/2}$ is the collapse timescale (with ρ_{h} the density of the halo at the time of collapse, see below). The factor $(a_{\text{coll}}/a_{\text{now}})^4$ accounts for the redshifting of the signal through cosmic expansion. The value of a_{coll} as a function of wave number will be determined further below. A halo of mass M corresponds to a structure characterized by a comoving wave-number k such that (assuming spherical symmetry)

$$M = \frac{4\pi}{3}(2\pi)^3 \frac{\rho_{\text{end}}}{H_{\text{end}}^3} \hat{k}^{-3}. \quad (41)$$

Therefore, the above equation can be rewritten as

$$\frac{d\Omega_{\text{gw}}^{\text{coll}}}{d \ln f} = \frac{\kappa}{3H_0^2} \frac{dn_{\text{h}}^{\text{coll}}}{d \ln M} \frac{d \ln M}{d \ln f} \mathcal{L}_{\text{gw}}^{\text{coll}} t_{\text{coll}} \left(\frac{a_{\text{coll}}}{a_0} \right)^4, \quad (42)$$

with f the comoving frequency of emission of gravitational waves, $f \simeq (2\pi t_{\text{coll}})^{-1}$, to be evaluated further below.

The luminosity $\mathcal{L}_{\text{gw}}^{\text{coll}}$ can be evaluated as follows [25]. The typical amplitude of a gravitational wave at point \mathbf{x} (the origin of the coordinates being chosen at the location of the emitting object) is given by the quadrupole formula which reads

$$h \simeq \frac{G}{2} \left(\ddot{I}_{ij} - \frac{1}{3} \ddot{I}_{kk} \delta_{ij} \right) \frac{n_i n_j}{|\mathbf{x}|}, \quad (43)$$

where $n_i \equiv x_i/|\mathbf{x}|$. The quantity in brackets is the trace free part of the quadrupole tensor I_{ij} . Since spherical motions do not generate gravitational waves, we need to assume that the halos are not spherically symmetric. A rough estimate of the quantity I_{ij} is

$$\ddot{I}_{ij} \simeq 2 \int_{\text{h}} \rho_{\text{h}} v_i v_j \simeq M v^2 \simeq \frac{2GM^2}{R}, \quad (44)$$

where R is the typical size of the halo (physical radius) at virialization and the virialized velocity $v_{\text{vir}} \simeq \sqrt{2GM/R}$. The luminosity of the source is thus given by

$$\mathcal{L}_{\text{gw}}^{\text{coll}} \simeq \frac{|\mathbf{x}|^2}{G} \dot{h}^2 \simeq \frac{G^4 M^5}{R^5}, \quad (45)$$

where we have written $\dot{h} \simeq h/T$ with $T \simeq R/v_{\text{vir}}$. The radius R is related to the wavenumber of the fluctuation by $R \equiv 2\pi a_{\text{coll}}/k$.

Formally, the number density of collapsed halos at a given time can be derived from a Press-Schechter mass function. With the above approximation at that all halos of mass M collapse instantaneously when the rms mass fluctuation on that scale exceeds δ_{c} , one derives the number density of halos of mass between M and $M + dM$ at collapse as

$$dn_{\text{h}}^{\text{coll}} \simeq \frac{\bar{\rho}(a_{\text{coll}})}{M} d \ln M \simeq \frac{\bar{\rho}(a_{\text{end}})}{M} \left(\frac{a_{\text{end}}}{a_{\text{coll}}} \right)^3 d \ln M, \quad (46)$$

with $\bar{\rho}(a_{\text{coll}})$ the mean density of the Universe at the time of collapse. This relation is nothing but the differential version of the equation $n_{\text{h}}/V = \bar{\rho}/M$ (V is the volume) which expresses the fact that, according to Press-Schechter, at a given time, most of the matter is contained in the halos that collapse at that time.

The rms mass fluctuation σ_M is related to σ_k , the root-mean-square of the Fourier amplitude of density perturbations via

$$\sigma_M^2 \simeq \int_0^k \frac{d^3 k'}{(2\pi)^3} \sigma_{k'}^2, \quad (47)$$

with k the comoving wave number of the perturbation enclosing a mass M defined in Eq. (41). In the last equation an approximation of simple k-space filtering has been applied, i.e. only modes $k' \leq k$ contribute to the average. Using Eq. (47) one finds

$$\sigma_M \approx \frac{1}{5} \mathcal{P}_{\zeta}(k)^{1/2} \frac{a}{a_{\text{end}}} \hat{k}^2. \quad (48)$$

Collapse of mass scale M occurs when $\sigma_M \simeq \delta_{\text{c}}$, hence at a collapse scale factor a_{coll} defined by

$$\frac{a_{\text{coll}}}{a_{\text{end}}} = 5 \delta_{\text{c}} \mathcal{P}_{\zeta}(k)^{-1/2} \hat{k}^{-2}. \quad (49)$$

At collapse, the typical over-density $\delta_{\text{coll}} \sim 150$ (in the spherical collapse model). The present day frequency is related to the comoving wave number of the perturbation as

$$\begin{aligned} f_0 &= \frac{1}{2\pi} \frac{a_{\text{coll}}}{a_0} H_{\text{coll}} (1 + \delta_{\text{coll}})^{1/2}, \\ &\simeq 3.8 \times 10^3 \text{ Hz } \hat{k} \left(\frac{T_{\text{rh}}}{10^9 \text{ GeV}} \right)^{1/3} \left(\frac{\mathcal{P}_{\zeta}}{10^{-11}} \right)^{1/4} \end{aligned} \quad (50)$$

Combining all the above, one ends up with

$$\begin{aligned} \frac{d\Omega_{\text{gw}}^{\text{coll}}}{d \ln f} &\sim 6 \times 10^3 \Omega_{\gamma,0} \frac{a_{\text{end}}}{a_{\text{rh}}} \mathcal{P}_{\zeta}^{5/4} \\ &\sim 2 \times 10^{-23} \hat{k}^{-2} \left(\frac{T_{\text{rh}}}{10^9 \text{ GeV}} \right)^{4/3} \left(\frac{\mathcal{P}_{\zeta}}{10^{-11}} \right)^{5/4} \end{aligned} \quad (51)$$

Maximum emission is provided by the largest scales that go non-linear at reheating, i.e those with wave number k_{nl} such that $a_{\text{coll}}(k_{\text{nl}}) = a_{\text{rh}}$. According to Eq. (49), this corresponds to

$$\hat{k}_{\text{nl}} \simeq 0.1 \left(\frac{T_{\text{rh}}}{10^9 \text{ GeV}} \right)^{2/3} \left(\frac{\mathcal{P}_{\zeta}}{10^{-11}} \right)^{-1/4}, \quad (52)$$

where we approximated $\mathcal{P}_{\zeta}(k_{\text{nl}}) = 10^{-11}$ in accord with Fig. 1. The frequency at maximum emission is thus

$$f_0^{\text{coll}} \simeq 3.7 \times 10^2 \text{ Hz } \left(\frac{T_{\text{rh}}}{10^9 \text{ GeV}} \right). \quad (53)$$

This falls in an interesting range considering the LIGO or BBO gravitational wave detectors. Nevertheless, the

signal is fairly weak: at the frequency of peak emission, one finds $d\Omega_{\text{gw}}^{\text{coll}}/d\ln f \sim 10^{-20}$ independent of reheating temperature, a signal which would be only very hard to detect. The signal as a function of frequency is represented in Fig. 2 in dotted line, annotated ‘‘collapse’’.

B. After initial collapse of halos

We have so far assumed that efficient GW emission in the non-linear regime happens only during the collapse phase of halos, up to the point where virialization is completed. It is not clear if post-virialization rotation/vibration of halos, potentially enhanced by occasional tidal forces acting on the halos due to passing by of other halos, may lead to further efficient emission of GWs. The question of how much more GWs are emitted after halo formation may only be addressed by complete numerical simulations and is beyond the scope of this paper. However, we may attempt to estimate it, introducing an efficiency parameter $\varepsilon < 1$, for emission of GWs after virialization. We may formally relate the generated GWs at times between the end of collapse and reheating $\rho_{\text{gw}}^{\text{coll}} >$ to $\rho_{\text{gw}}^{\text{coll}}$ in Eq. (40) by making the following replacements in Eq. (40): $\rho_{\text{gw}}^{\text{coll},0} \rightarrow \rho_{\text{gw}}^{\text{coll},0} >$, $dn_h(M) \rightarrow dn_h^{\text{coll}} >(M) = dn_h(M)(a_{\text{coll}}/a)^3$ to take into account the fact that the signal is emitted after the collapse, $\mathcal{L}_{\text{gw}}^{\text{coll}} \rightarrow \mathcal{L}_{\text{gw}}^{\text{coll}} > = \varepsilon \mathcal{L}_{\text{gw}}^{\text{coll}}$ as discussed above, and, finally, $t_{\text{coll}} \rightarrow t_{\text{coll}} > = t_{\text{coll}}(a/a_{\text{coll}})^{3/2}$, $(a_{\text{coll}}/a_0)^4 \rightarrow (a/a_0)^4$, again to take into account that the emission time is now different. Inserting this into Eq. (40) yields

$$d\rho_{\text{gw}}^{\text{coll},0} > \approx d\rho_{\text{gw}}^{\text{coll},0} \left(\frac{a}{a_{\text{coll}}} \right)^{5/2} \varepsilon, \quad (54)$$

implying a potentially large enhancement of the signal when $a_{\text{rh}} \gg a_{\text{coll}}$, provided ε is not too small. Using this in conjunction with Eq. (51) one finds that for non-negligible ε the signal may be dominated by the emission of GWs at T_{rh} from the first structures which had formed. One would then expect a signal $d\Omega_{\text{gw}}/d\ln f \sim 2 \times 10^{-18} \varepsilon (T_{\text{rh}}/10^9 \text{ GeV})^{-2} (\mathcal{P}_\zeta/10^{-11})^{5/2}$ with a rather strong dependence on the reheating temperature, which would make it potentially detectable (provided ε is not too small, of course): for $T_{\text{rh}} \sim 10^6 \text{ GeV}$, the signal becomes of order 10^{-12} in the 10^{-2} Hz range. Assuming indeed that the typical pulsation corresponds to the Hubble scale at the time of emission, one finds a frequency $f_0^{\text{coll}} > \sim 30 \text{ Hz} (T_{\text{rh}}/10^9 \text{ GeV})$ for the peak emission at T_{rh} . This signal is indicated by the ‘‘merger’’ upper limit in Fig. 2, given the uncertainty on the value of ε .

C. Evaporation of halos

Around the epoch of reheating, the self-gravitating halos evaporate due to emission of radiation by the decaying inflaton. Due to the smallness of the inflaton-radiation

coupling, the radiation does not scatter on the inflaton particles contained in the halos, but escapes freely without communicating its pressure to the inflaton halo. In this picture, each halo behaves as a source of radiation with a typical emission timescale $\tau_\phi = \Gamma_\phi^{-1}$ corresponding to the inflaton lifetime. The mean free path of radiation against scattering with itself is $\lambda \sim 1/(\alpha^2 T)$, with α a typical coupling constant and T the temperature of the radiation, therefore $\lambda \ll \tau_\phi$ and the radiation can be approximated as an instantaneously thermalized ultra-relativistic fluid. The radiation emitted by the evaporating halo expands and accelerates under its own internal pressure until it interacts with the winds emitted by surrounding halos. We will address this phase in the following subsection and for the time being, we estimate the amount of gravitational waves produced during the evaporation of the halos, taken individually.

Since the radiation escapes on a timescale $t_{\text{esc}} = R/c$, with R the radius of the virialized halo, and since $R \ll H^{-1}$, the hierarchy $t_{\text{esc}} \ll \tau_\phi$ remains satisfied all throughout evaporation. This implies that the energy of radiation contained in the halo at any time, $M t_{\text{esc}}/\tau_\phi$ is always smaller than M , so that its gravitational influence can be neglected.

As the halo evaporates, its virial radius increases in inverse proportion to M . In order to see this, one first notices that the dynamical timescale of evolution of the halo, $t_{\text{dyn}} = (\kappa \rho_h/3)^{-1/2}$ remains much smaller than the Hubble time $(\kappa \rho/3)^{-1/2}$ during the evaporation process, since $\rho_h \gg \rho$. Therefore the structure adjusts itself on a timescale which is much smaller than the evaporation timescale $\tau_\phi = H_{\text{rh}}^{-1}$ (H_{rh}^{-1} the Hubble time at reheating). In other words, the halo undergoes a series of quasi-static equilibria as the mass decreases, the virial relation $M v^2 \simeq 2GM^2/R$ being verified at each step. Through adiabatic expansion, the rms velocity decreases as $1/R$, hence one can check that $dM/M = -dR/R$.

During evaporation, the luminosity can be expressed as [25]

$$\mathcal{L}_{\text{gw}} \simeq \bar{\varepsilon} G \left(\frac{dM}{dt} \right)^2. \quad (55)$$

Here $\bar{\varepsilon} < 1$ is an efficiency factor which represents a measure of the asphericity of the radiation wind, analogous to the factor introduced in Section IV B. Using the previous arguments, the amount of energy density emitted in gravitational waves on an evaporation timescale τ_ϕ approximately reads:

$$\begin{aligned} d\rho_{\text{gw}} &\simeq \bar{\varepsilon} \frac{G}{4} \left(\frac{dM}{dt} \right)^2 \tau_\phi dn_{h|\text{rh}}(M) \\ &\simeq \bar{\varepsilon} \frac{G}{2} M^2 H_{\text{rh}} dn_{h|\text{rh}}(M) \end{aligned} \quad (56)$$

where $dn_{h|\text{rh}}$ is the number density of halos of mass comprised between M and $M + dM$ at the time of reheating and $H_{\text{rh}} \simeq 1/(2\tau_\phi)$ denotes the Hubble scale at reheating. It is important to note that all halos evaporate

on the same timescale τ_ϕ , therefore they all contribute to the gravitational wave signal at the same comoving pulsation $\sim a_{\text{rh}}\tau_\phi^{-1}$. Due to the quadratic dependence on mass scale M the signal is dominated by the largest structures evaporating. This is given by the typical mass scale which collapses shortly before reheating. It may be obtained by employing Eq. (49) with $a_{\text{coll}} \approx a_{\text{rh}}$ yielding the final simple result

$$\Omega_{\text{gw}} \sim \bar{\varepsilon} \Omega_{\gamma,0} P_\zeta(k_{\text{nl}})^{3/4}, \quad (57)$$

independent of reheating temperature. The typical frequency of emission corresponds to the (redshifted) Hubble scale of reheating (divided by 2π) and is given as before by $f_0^{\text{coll}} \sim 30 \text{ Hz} (T_{\text{rh}}/10^9 \text{ GeV})$, in an interesting range from the point of view of detection.

The above signal may be quite substantial, in particular, for $P_\zeta \sim 10^{-11}$ as implied by Fig. 1 one obtains $\Omega_{\text{gw}} \sim 4 \times 10^{-13} \bar{\varepsilon}$. Of course, the signal may be smaller than our estimate in case velocities are below the speed of light and/or $\bar{\varepsilon} \ll 1$.

D. Dissipation after reheating

As explained above, once the radiation is emitted, it will shock against the radiation generated by surrounding halos. All in all, this injects a large amount of energy on all scales $\lesssim L_s \equiv 2\pi a_{\text{rh}}/k_{\text{nl}}$, where k_{nl} denotes as before the smallest comoving wave number of perturbations that go non-linear by reheating. On general grounds, one expects that this injection of energy stirs a turbulent cascade on scales $\lesssim L_s$, which decays through damping at small scales. This cascade is characterized by a power spectrum of kinetic energy in modes (eddies) of various wave numbers, which can emit gravitational radiation in the very same way that growing perturbations do during the linear phase. This has been discussed in detail by Kosowsky *et. al* [10] and we simply adapt their calculation to the present framework. We may assume here that a fraction of order unity of the total energy density at reheating is injected in the cascade, *i.e.* kinetic energy of the radiation fluid is of order the rest energy. The stirring scale L_s can be evaluated by using Eq. (49), with $a_{\text{coll}} = a_{\text{rh}}$, which yields

$$L_s \simeq 2 \mathcal{P}_\zeta^{1/4} H_{\text{rh}}^{-1}. \quad (58)$$

The stirring scale is much smaller than the timescale $\tau_\phi \sim H_{\text{rh}}^{-1}$ over which energy is injected into the plasma, so that one may consider the turbulence to be stationary over this timescale τ_ϕ . Following [10], one then finds that the gravitational wave signal generated is:

$$\begin{aligned} \frac{d\Omega_{\text{gw}}}{d \ln f} &\sim 2 \times 10^{-7} \left(\frac{\tau_\phi}{H_{\text{rh}}^{-1}} \right)^{-1} \left(\frac{L_s}{H_{\text{rh}}^{-1}} \right)^3 \left(\frac{f}{f_s} \right)^{-7/2}, \\ &\sim 2 \times 10^{-14} \left(\frac{\mathcal{P}_\zeta}{10^{-11}} \right)^{3/4} \left(\frac{f}{f_s} \right)^{-7/2}, \end{aligned} \quad (59)$$

independent of reheating temperature. The typical frequency is defined as

$$\begin{aligned} f_s &= \frac{1}{3\pi} \frac{a_{\text{rh}}}{a_0} (\tau_\phi L_s^2)^{-1/3} \\ &= 10^3 \text{ Hz} \left(\frac{T_{\text{rh}}}{10^9 \text{ GeV}} \right) \left(\frac{\mathcal{P}_\zeta}{10^{-11}} \right)^{-1/6}. \end{aligned} \quad (60)$$

Although not as strong as that resulting from the evaporation of halos, this signal remains substantial and the typical frequency can easily shift down to the interesting range for detection if the reheating temperature $T_{\text{rh}} \lesssim 10^7 \text{ GeV}$. This signal is indicated in Fig. 2 by the dashed-dotted line annotated ‘‘turbulence’’.

V. CONCLUSION

In this paper we have calculated the gravitational wave signal associated to the growth of sub-horizon perturbations between the end of cosmic inflation and the beginning of a radiation dominated early Universe in $m^2\phi^2$ chaotic inflation. The growth of metric fluctuations formally arises from a preheating like instability and can be interpreted, in the range of wave numbers of interest, as the gravitational instability of a pressure-less fluid in a matter dominated era. The over-density $\delta\rho_{\mathbf{k}}/\rho$ of these perturbations grows linearly with scale factor and reach non-linearity to re-collapse and form inflaton halos after only moderate expansion of the Universe.

Though these small-scale inflaton halos later evaporate when the inflaton decays at reheating, they may nevertheless lead to the emission of gravitational waves in an interesting frequency range $\omega_0 \sim 10^{-5} - 10^8 \text{ Hz}$ for current ground-based and planned satellite gravitational wave detectors, such as Advanced LIGO, DECIGO and BBO. We have therefore analyzed the gravitational wave emission in detail during five distinct phases: (a) growth of the linear perturbations, (b) first collapse of halos when reaching non-linearity, (c) subsequent non-linear evolution of halos, (d) evaporation of halos due to inflaton decay, and (e) cosmic turbulence during the first epochs of radiation domination, respectively. We note here that phase (a) has recently also been studied by Ref. [21]. An exact calculation of (a) indicates that gravitational wave emission is weak, peaking at values of order $\Omega_{\text{gw}} \sim 10^{-22} T_{\text{rh}}^{-4/3}$, if the magnitude of curvature perturbations on small scales as predicted in chaotic inflation, *i.e.* $\mathcal{P}_\zeta \sim 10^{-11}$, is assumed. The estimate of gravitational wave emission during phase (b) is similarly small. Promising gravitational wave signals of $\Omega_{\text{gw}} \gtrsim 10^{-12}$ for $P_\zeta \sim 10^{-11}$, could however, result during phases (c) (d) and (e), depending on the value of the reheating temperature. Generally speaking, the lower the reheating temperature, the longer the phase of growth of fluctuations and the larger the band of wave numbers turning non-linear, and consequently, the larger the signal of gravitational wave emission. The exact value of these signals

depends on the details of the structure formation process including tidal disruption of substructures, rotation, as-

phericity, etc. A reliable estimate may therefore only be given when full numerical simulations are performed.

-
- [1] F. R. Bouchet, (2009), 0911.3101.
 - [2] V. Corbin and N. J. Cornish, *Class. Quant. Grav.* **23**, 2435 (2006), gr-qc/0512039.
 - [3] S. Kawamura *et al.*, *Class. Quant. Grav.* **23**, S125 (2006).
 - [4] A. Kosowsky, M. S. Turner, and R. Watkins, *Phys. Rev. Lett.* **69**, 2026 (1992).
 - [5] A. Kosowsky, M. S. Turner, and R. Watkins, *Phys. Rev.* **D45**, 4514 (1992).
 - [6] A. Kosowsky and M. S. Turner, *Phys. Rev.* **D47**, 4372 (1993), astro-ph/9211004.
 - [7] M. Kamionkowski, A. Kosowsky, and M. S. Turner, *Phys. Rev.* **D49**, 2837 (1994), astro-ph/9310044.
 - [8] A. Nicolis, *Class. Quant. Grav.* **21**, L27 (2004), gr-qc/0303084.
 - [9] C. Grojean and G. Servant, *Phys. Rev.* **D75**, 043507 (2007), hep-ph/0607107.
 - [10] A. Kosowsky, A. Mack, and T. Kahniashvili, *Phys. Rev.* **D66**, 024030 (2002), astro-ph/0111483.
 - [11] A. D. Dolgov, D. Grasso, and A. Nicolis, *Phys. Rev.* **D66**, 103505 (2002), astro-ph/0206461.
 - [12] G. Gogoberidze, T. Kahniashvili, and A. Kosowsky, *Phys. Rev.* **D76**, 083002 (2007), 0705.1733.
 - [13] S. Y. Khlebnikov and I. I. Tkachev, *Phys. Rev.* **D56**, 653 (1997), hep-ph/9701423.
 - [14] R. Easther and E. A. Lim, *JCAP* **0604**, 010 (2006), astro-ph/0601617.
 - [15] R. Easther, J. T. Giblin, Jr., and E. A. Lim, *Phys. Rev. Lett.* **99**, 221301 (2007), astro-ph/0612294.
 - [16] J. Garcia-Bellido and D. G. Figueroa, *Phys. Rev. Lett.* **98**, 061302 (2007), astro-ph/0701014.
 - [17] J. Garcia-Bellido, D. G. Figueroa, and A. Sastre, *Phys. Rev.* **D77**, 043517 (2008), 0707.0839.
 - [18] J. F. Dufaux, A. Bergman, G. N. Felder, L. Kofman, and J.-P. Uzan, *Phys. Rev.* **D76**, 123517 (2007), 0707.0875.
 - [19] M. Maggiore, *Phys. Rept.* **331**, 283 (2000), gr-qc/9909001.
 - [20] K. Jedamzik, M. Lemoine, and J. Martin, (2010), 1002.3039.
 - [21] H. Assadullahi and D. Wands, *Phys. Rev.* **D79**, 083511 (2009), 0901.0989.
 - [22] LIGO, B. Abbott *et al.*, *Astrophys. J.* **659**, 918 (2007), astro-ph/0608606.
 - [23] LIGO Scientific, J. R. Smith, *Class. Quant. Grav.* **26**, 114013 (2009), 0902.0381.
 - [24] K. Nakayama, S. Saito, Y. Suwa, and J. Yokoyama, *JCAP* **0806**, 020 (2008), 0804.1827.
 - [25] B. F. Schutz, *American Journal of Physics* **52**, 412 (1984).